Analysis of Nonlinear Hepatic Clearance of a Cyclopentapeptide, BQ-123, with the Multiple Indicator Dilution Method Using the Dispersion Model

Akihiro Hisaka,[1,4] Tatsuji Nakamura,[2] and Yuichi Sugiyama[3]

Received June 20, 1998; accepted October 5, 1998

Purpose. To bridge *in vitro, in situ* and *in vivo* kinetic analyses of the hepatic clearance of a cyclopentapeptide, BQ-123, by using dispersion models that assume nonlinear pharmacokinetics.

Methods. Rat livers were perfused by the multiple indicator dilution method with doses of BQ-123 ranging from 1-1000 μg. The outflow dilution curves were fitted to a two-compartment dispersion model that was solved numerically by the finite difference method. Further, *in vivo* plasma concentrations of BQ-123 after bolus injection were analyzed with a hybrid physiological model that incorporates the hepatic dispersion model.

Results. The calculated Michaelis-Menten constants (K_m = 12.0 μM, V_{max} = 321 pmol/min/10^6 cells, P_{dif} = 1.2 μl/min/10^6 cells) were comparable to those obtained previously from the *in vitro* isolated hepatocyte experiment (K_m = 9.5 μM, V_{max} = 517 pmol/min/10^6 cells, P_{dif} = 1.1 μl/min/10^6 cells). The plasma concentrations of BQ-123 at doses of 1–25 mg/kg were explained well by the hybrid physiological model.

Conclusions. These results suggest that carrier-mediated transport on the sinusoidal membrane was responsible for the *in vivo* hepatic elimination of BQ-123.

KEY WORDS: nonlinear pharmacokinetics; dispersion model; multiple indicator dilution method; BQ-123; hepatic transport; finite difference method.

INTRODUCTION

Non-steady-state liver perfusion by the multiple indicator dilution (MID) method is appropriate for analyzing various processes in the liver because it can differentiate sinusoidal influx and efflux of substances (1–4). An advantage of a perfusion study is that the physiology of the liver is maintained. However, to evaluate the hepatic clearance of drugs, *in vitro* isolated or cultured hepatocyte experiments are generally preferred over perfusion studies. This is not only because of experimental difficulties with perfusion, but also because of methodological difficulties in analyzing non-steady-state perfusion. It is a challenging issue to analyze nonlinear pharmacokinetics with MID data.

Goresky *et al.* proposed injecting a trace bolus dose of a radio-labeled compound into a liver being perfused constantly with various concentrations of the non-labeled compound to analyze nonlinear pharmacokinetics (1,5). In this method, dynamic change of the drug concentration in the organ can be ignored; accordingly, the analysis becomes simple. The disposition of bromosulfophthalein-glutathione in the liver was analyzed by this method, and it was found that various factors, not only transporters and metabolizing enzymes but also saturable binding with intracellular proteins, govern the nonlinearity of the hepatic clearance (3). This method has been useful to gain insights into the behavior of drugs in the liver; however, the experimental technique is rather circuitous for routine use.

Uptake of serotonin by the lung was analyzed in a more straightforward manner by Malcorps *et al.* (6). They analyzed the MID data of various bolus doses directly by the distributed tube model (without background constant infusion). However, the bolus input is a difficult precondition for the distributed tube model because the drug concentrations are estimated as infinity by the model due to lack of micro-mixing (7,8). To avoid this problem, Malcorps *et al.* approximated pre-dispersion of the drug before perfusate enters the liver (6). It should be noted that the extent of the approximated pre-dispersion has a significant influence on the analysis.

In contrast to the distributed tube model, the dispersion model assumes micro-mixing of the blood stream *a priori* (7). Since it was proposed by Roberts *et al.* (9,10), the dispersion model has been used frequently to analyze MID data (11,12). Although the model has been criticized in terms of its mathematical complexity (13), the problem can be overcome by applying numeric calculation methods such as the fast inverse Laplace transform (FILT) method (11), and more recently, the finite difference method (FDM) (14,15). In the present study, MID experiments of a test drug were performed in a manner similar to that of Malcorps *et al.*, but the data were analyzed with the dispersion model solved by FDM.

BQ-123, a cyclopentapeptide, was used as the test compound. BQ-123, which is the first reported selective antagonist of the endothelin A receptor (16), is frequently used to elucidate the biology of endothelin (17,18). The compound has therapeutic potential (18,19); however, its very short plasma half-life (2–4 min in rats) hinders practical clinical use (20). BQ-123 is not metabolized in the body and is excreted rapidly into the bile in unchanged form (20). BQ-123 is taken up into isolated rat hepatocytes very efficiently by a carrier-mediated active transport mechanism (20). In addition, BQ-123 is transported across the bile canalicular membrane in an ATP-dependent manner (21). This canalicular transport is deficient in EHBR rats (21), suggesting the involvement of cMOAT, an MRP transporter family protein (22–24). In this study, we analyzed these contributions quantitatively with the aid of the dispersion model. Preliminary analysis of the MID study of BQ-123 was reported previously (14).

[1] Development Research Laboratories, Banyu Pharmaceutical Co. Ltd., 810, Nishijo, Menuma-Machi, Osato-Gun, Saitama 360-0214, Japan.
[2] Tsukuba Research Laboratories, Banyu Pharmaceutical Co. Ltd., 3, Okubo, Tsukuba, Ibaraki 300-2611, Japan.
[3] Faculty of Pharmaceutical Sciences, University of Tokyo, 3-1, Hongo 7, Bunkyo-ku, Tokyo 113-0033, Japan.
[4] To whom correspondence should be addressed. (e-mail: hisakaah@banyu.co.jp)

ABBREVIATIONS AIC, Akaike's information criteria; BSA, bovine serum albumin; FDM, finite difference method; FID, fluoresceine isothiocyanate dextran; FILT, fast inverse Laplace transform; MID, multiple indicator dilution.

0724-8741/99/0100-0103$16.00/0

MATERIALS AND METHODS

Chemicals and Reagents

Unlabeled BQ-123 (sodium cyclo[D-Trp-D-Asp-L-Pro-D-Val-L-Leu]) was synthesized at the Tsukuba Research Institute of Banyu Pharmaceutical Co. Ltd. (Tsukuba, Japan). ^{3}H-BQ-123 was obtained from Amersham (Buckinghamshire, UK). Fluoresceine isothiocyanate dextran (FID, average molecular weight 40500) was purchased from Sigma Chemical (St. Louis, MO, USA). Water was purified with the MilliQ system (Millipore, USA). All other chemicals and reagents were commercial products of analytical grade.

In Situ Liver Perfusion Study

Single-pass liver perfusion was performed by the Mortimore method (4,14). Briefly, male Sprague-Dawley rats (7–8 weeks, 250–350 g, Charles River Japan, Tokyo, Japan) were anaesthetized with ketamine (235 mg/kg) and xylazine (2.3 mg/kg), and the liver was perfused from the portal vein with oxygenated Krebs-Ringer-bicarbonate buffer containing 10 mM D-glucose and 2% bovine serum albumin (BSA). The perfusate flow rate was 32–33 ml/min. Continuous secretion of the bile was regarded as an indicator of liver viability. After a stabilization period of 10 min, 200 μl of the perfusate containing ^{3}H-BQ-123 and 50 μg of FID as an extracellular reference was injected into the system. The eluate from the cannula inserted into the hepatic vein was fractionated at 0.83-sec intervals over 30 sec to holes on a turntable. Radioactivity in the eluate was measured by liquid scintillation counting. The concentration of FID was measured as previously reported (14). The dilution curves were not corrected for the void volume of the cannula in this study. Instead, lag time was calculated by fitting analysis.

Protein Binding

The protein binding of BQ-123 to 2% BSA in 10 mM phosphate buffer-saline (pH 7.4) was determined by an ultrafiltration method as reported previously (20). The protein binding of BQ-123 to 2% BSA was 27%.

Nonlinear Dispersion Model

The dispersion model is a stochastic model which assumes that movements of a solute by the blood stream flowing through the heterogeneous micro-capillaries are describable in terms of the dispersion (9,10). The general equation of the one- and two-compartment model (7,11) is expressed by the following partial differential equations for the drug concentrations in the liver (10,14):

$$\frac{\partial C_{HB}}{\partial t} = \frac{D_N Q_H}{V_{HB}} \frac{\partial^2 C_{HB}}{\partial Z^2} - \frac{Q_H}{V_{HB}} \frac{\partial C_{HB}}{\partial Z} + Tr_{HB}(C_{HB}, C_{HT}) \quad (1)$$

$$\frac{\partial C_{HT}}{\partial t} = Tr_{HT}(C_{HB}, C_{HT}) \quad (2)$$

where C_{HB} and C_{HT} are drug concentrations in the hepatic blood vessel and hepatic tissue, respectively, V_{HB} is the volume of the hepatic blood vessel that includes Disse space, D_N is the normalized dispersion coefficient, Q_H is the hepatic blood flow rate, t is time, and Z is the dimensionless axial coordinate from the entrance of the liver. Equations 1 and 2 have occasionally been represented in a dimensionless form in the literature (10,11), but we used them as they were to retain flexibility in performing the simultaneous fitting. The characteristics of the model depend on $Tr_{HB}()$ and $Tr_{HT}()$, which represent the disappearance and/or exchanging of the drug in the hepatic blood vessel and tissue, respectively. A detailed description of Models 1–4 tested in this study is given in Scheme 1a.

Nonlinear Least Squares Fitting of MID Data

The simulation and fitting of the experimental data were performed by a multi-purpose nonlinear regression program, Napp (14). The program generates dilution curves of the closed boundary conditions by the finite difference method (FDM).

The dilution curves at all doses were simultaneously fitted to the model. The kinetic parameters K_m, V_{max}, k_{10}, k_{20}, k_{12} and k_{21} (see Scheme 1 for definitions) were assumed to apply to all dilution curves, while D_N, V_B and lag time were allowed to take independent values. When the dilution curves of FID (the vascular reference) were simultaneously fitted, D_N and lag time were linked in a corresponding pair (BQ-123 and FID) but were allowed to be free from the other curves. The ratio of V_{HB} of BQ-123 to that of FID were adjusted to be the same for all dilution curves. The dilution curves of FID were fitted to the 2-compartment model, and its k_{12} and k_{21} were allowed to be independent from those of BQ-123. These complicated conjunctions of the parameters were realized by using Napp's automatic model-generation feature for simultaneous fitting (14).

The damping Gauss-Newton algorithm and half reciprocal weight (1/Y) were used unless otherwise noted for nonlinear regression analysis. For simultaneous fitting of multiple data sets, weight balancing was adopted to compensate for the differences in values and sample size between each set of data (14).

Hybrid Physiological Model

To simulate the plasma levels of BQ-123 *in vivo*, a hybrid physiological model was constructed. Schematic representation of the model is shown in Scheme 1b. For the liver, a 1-compartment nonlinear dispersion model, Model 1 (Scheme 1a), was assumed. For systemic blood and tissue, the following differential equations were adopted,

$$V_B \frac{dC_B}{dt} = Q_H(C_{HB,exit} - C_B) + CL_T C_T - (CL_B + \frac{1}{R_B} CL_{R,plasma}) C_B \quad (3)$$

$$V_T \frac{dC_T}{dt} = CL_B C_B - CL_T C_T \quad (4)$$

where V_B, V_T, CL_B and CL_T are the distribution volumes and distribution clearances for the blood and peripheral tissue, respectively, R_B is the blood to plasma concentration ratio (0.6 (20)), $CL_{R,plasma}$ is the renal plasma clearance (6 ml/min/kg (20)), C_T is the concentration of the drug in peripheral tissue, and $C_{HB,exit}$ is the blood concentration at the exit of the liver calculated by the dispersion model. The above equations were combined and integrated numerically by the rational Runge-Kutta method (14), and drug concentration versus time profiles were obtained.

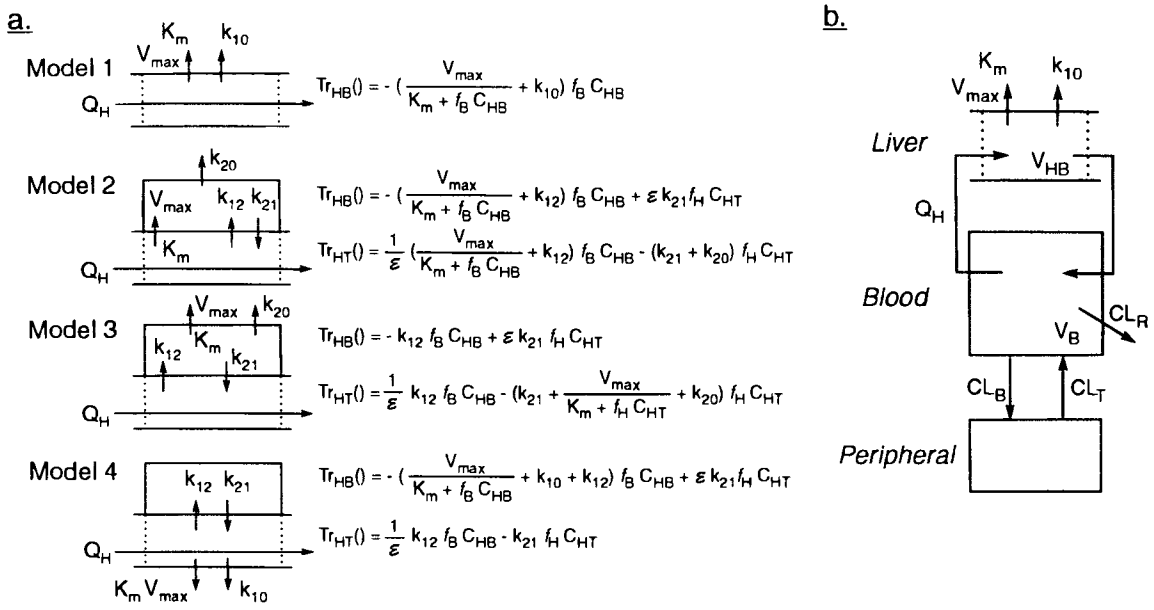

Scheme 1. Structure of the nonlinear dispersion models (a), and the hybrid physiological model (b). K_m and V_{max} are the Michaelis-Menten constants for nonlinear transport or sequestration; k_{10}, k_{12}, k_{21}, and k_{20} are the first-order rate constants; f_B and f_T are the unbound fractions of the drug in blood and hepatic tissue, respectively; V_{HB} is the distribution volume of blood in the liver; and ε is the ratio of the distribution volume for the hepatic tissue to V_{HB}. For further information, refer to Materials and Methods.

To adapt the model to the actual plasma levels, nonlinear least squares fitting was performed as described for MID data. Plasma levels after the intravenous injection of three doses of BQ-123 (20) were simultaneously fitted to the model by adjusting parameters Q_H, V_B, CL_B and CL_T. The other parameters were fixed to the values obtained in the liver perfusion study.

Calculation of Kinetic Parameters for Isolated Rat Hepatocytes

We previously reported the kinetic parameters for the carrier-mediated uptake of BQ-123 into isolated rat hepatocytes (20). The K_m values were 5.9 and 12.1 μM for Na^+-dependent and Na^+-independent uptake, respectively. In the present study, we combined these two uptakes to simplify the analysis. The combined kinetic parameters were newly calculated by nonlinear least squares fitting of the uptake data reported previously (20).

RESULTS

In Situ Liver Perfusion Study

The analysis of the mean outflow dilution curves of BQ-123 at doses of 1, 10, 100 and 1000 μg in the MID studies is shown in Fig. 1. Hepatic extraction of BQ-123 was saturable as evidenced by increasing availability from 42% at 1 μg to 91% at 1000 μg. The dilution curves of FID (the vascular reference) were independent of the dose of BQ-123. Fig. 1d shows the ratio plot, a logarithmic plot of the ratio of FID to BQ-123. The shape of the plot depressed as the dose increased. This has been reported as a characteristic of nonlinear kinetics (6,14,15).

The mean dilution curves of BQ-123 were analyzed with the nonlinear dispersion models shown in Scheme 1. Model 1, a 1-compartment model and the simplest method, explained the saturation reasonably, although it could not describe the tail part of the dilution curves (Fig. 1a). Model 2 gave a moderately good approximation but some systematic errors remained (Fig. 1b), suggesting disagreement between the data and the model. Model 3 failed to fit to the data by any means. Model 4 explained the experimental data most satisfactorily as judged from the lowest Akaike's information criteria (AIC) value (25) (Table 1, Fig. 1c). Model 4 is a 2-compartment model, but the sequestration is assumed to occur from the blood compartment. From these data, we concluded that Model 4 was the most appropriate model to describe the local pharmacokinetics of BQ-123 in rat liver but Model 1 was acceptable in some cases to estimate availability.

Analysis of the mean dilution curves was helpful in selecting the model; however, the obtained parameters were not very reliable. This is because the dilution curves varied considerably from animal to animal (the CV values of the mean dilution curves were approximately 50%). We assumed that the variance was enhanced by the differences in the distribution volume and the extent of approximate dispersion. To overcome this problem, simultaneous fitting of 12 sets of individual dilution curves was performed, and it was found that Model 4 explained all of the dilution curves satisfactorily (Table 2 and Fig. 2). The values of the parameters were compared with those obtained in the isolated hepatocyte study (Table 3). Although V_{max} was moderately lower in the perfusion study, K_m and P_{dif} were in excellent agreement.

Without using the dilution curves of FID, some of parameters D_N and V_{HB} were difficult to estimate due to scattering. The fitting worsened by fixing V_{HB}, or k_{12} and k_{21} of FID to

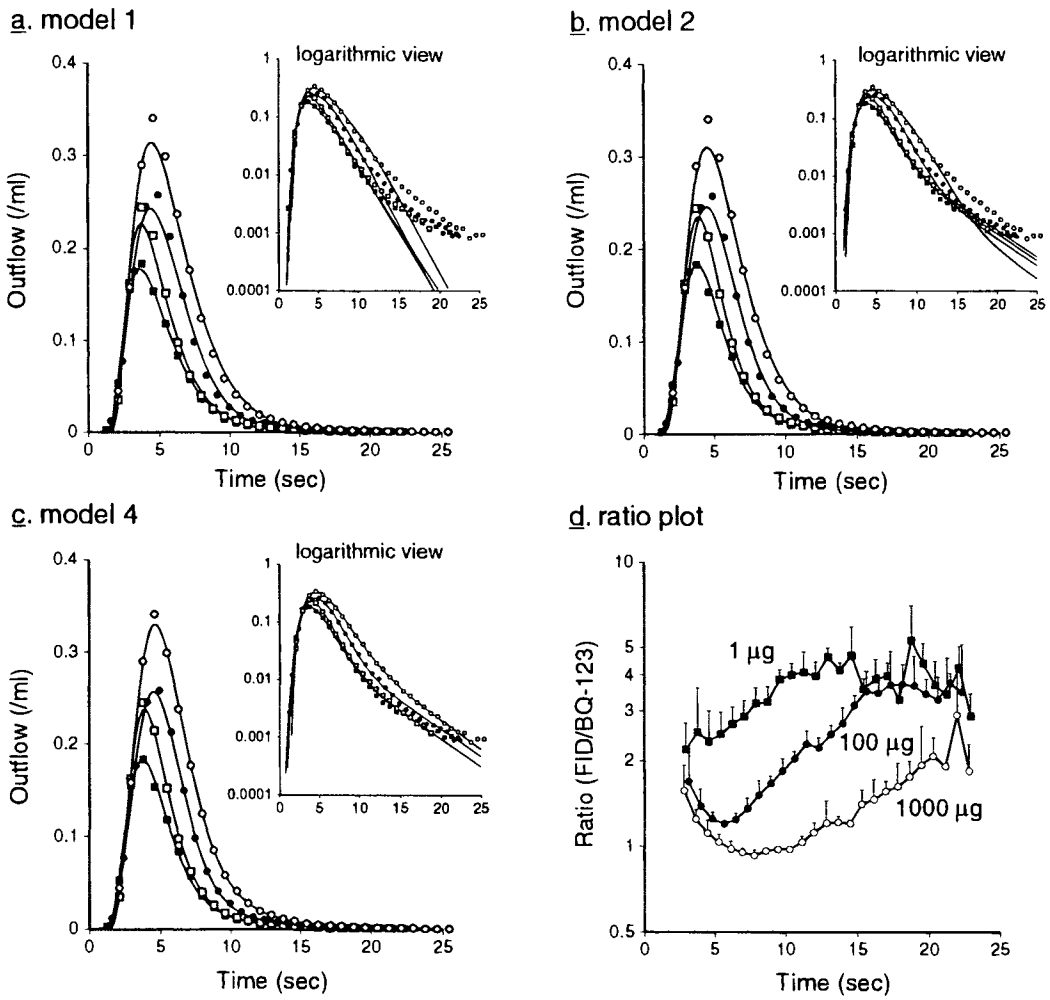

Fig. 1. Schematic representation of least squares fitting analysis of mean dilution curves of BQ-123 to Model 1 (a), Model 2 (b), and Model 4 (c), and (d) ratio of FID (vascular reference) to BQ-123 in the perfusate. Each point is the mean of three perfusions at a dose of 1 μg (closed squares), 10 μg (open squares), 100 μg (closed circles), and 1000 μg (open circles). In panel (d), the curve for the dose of 10 μg was omitted for clearer representation.

the corresponding values for BQ-123. The fitting also worsened when k_{10} was omitted from the model (data not shown), suggesting that the hepatic extraction of BQ-123 consists not only of a saturable component but also of a linear component.

Analysis with the Hybrid Physiological Model

Plasma levels of BQ-123 after intravenous injection of the compound in rats (20) were fitted to a hybrid physiological model in which the nonlinear dispersion model was incorporated for hepatic clearance (Fig. 3). In this analysis, K_m, V_{max} and k_{10} obtained from the *in situ* liver perfusion study were used. The plasma levels of three doses were explained well by the model, indicating that the non-linearity of CL_{tot} observed *in vivo* was ascribable to the saturation of hepatic uptake observed in the perfusion study.

Table 1. Fitting of Various Models to the Mean Outflow Dilution Curves of BQ-123 in Perfused Rat Liver

	Model 1	Model 2	Model 3	Model 4
# of parameters	15	17	17	17
Weight	1	1	1	1
ss	0.00812	0.00286	−[a]	0.00066
AIC[b]	−461	−563	−[a]	−713

Note: The structure of the models was shown in Scheme 1.
[a] The calculation did not converge.
[b] Akaike's information criteria.

DISCUSSION

The dilution curves of BQ-123 were fitted most satisfactorily to Model 4 (Fig. 1), in which the saturable sequestration occurred directly from the blood compartment, suggesting that the rate-limiting step of hepatic elimination was sinusoidal transport from the blood to hepatocytes. The meaning of the second compartment was not determined in this study. We surmise that the second compartment represents the adsorption of the drug to the surface of the micro-capillaries or cells. Considering the similarity in the shape of the curves, the reason for the bi-phasic decline of FID may be the same as for BQ-123. Temporal adsorption of a drug to the surface of the perfused liver has been reported previously (26).

Table 2. Simultaneous Nonlinear Least Squares Analysis of Outflow Dilution Curves of BQ-123

# of parameters	44
# of data sets	12
# of sampling points	619
weight	1
K_m (μM)	12.0 ± 0.9
V_{max} (μM/min)	186 ± 14
k_{10} (/min)	0.69 ± 0.15
k_{12} (/min)	2.1 ± 0.1
$\varepsilon f_H k_{21}$ (/min)	12.7 ± 0.6
$(f_B k_{12})_{FID}$ (/min)	2.6 ± 0.1
$(\varepsilon f_H k_{21})_{FID}$ (/min)	14.5 ± 0.4
D_N	0.093 ± 0.034[a]
V_{HB} (ml)	2.87 ± 0.44[a]
$V_{HB}/(V_{HB})_{FID}$	1.12 ± 0.01
Lag time (sec)	0.58 ± 0.58[a]

Note: Individual dilution curves of BQ-123 and FID were fitted to a nonlinear two-compartment dispersion model (Model 4). See Scheme 1 for definitions of the parameters.

[a] The mean and s. d. of twelve estimated parameters.

Table 3. Michaelis-Menten Constants of Hepatic Uptake of BQ-123 in Rats

Method	K_m (μM)	V_{max} (pmol/min/10^6 cell)	P_{dif} ($k_{10} \cdot V_{HB}$) (μl/min/10^6 cell)
Isolated hepatocyte	9.5	517	1.1
Liver perfusion	12.0	321[a,b]	1.2[a,c]

[a] The following values were adopted to calculate the parameters: body weight 0.3 kg, liver weight 44.4 g/kg, number of liver cells 1.25 × 10^8 /g liver.

[b] 321 (pmol/min/10^6 cell) = 186 (μM/min) × 2.87 (ml) × 10^9 / 1.25 × 10^8 / 44.4 / 0.3.

[c] 1.2 (μl/min/10^6 cell) = 0.69 (/min) × 2.87 (ml) × 10^9 / 1.25 × 10^8 / 44.4 / 0.3.

The Michaelis-Menten constants (K_m and V_{max}) obtained from the MID study were comparable to those from the isolated hepatocyte study (Table 3), indicating that the sinusoidal transport observed in the hepatocyte experiment plays a fundamental role in the physiological liver. The reason for the moderate difference in V_{max} is unclear. To clarify this issue, we probably need to take into consideration various factors such as the perfusion rate, protein binding, the viability of the perfused liver, and the physiological conditions of the hepatocytes.

Using a hybrid model, we demonstrated that the plasma concentration versus time profiles of BQ-123 after various intravenous doses were kinetically explainable by the saturation of hepatic uptake observed *in vitro* and *in situ* (Fig. 3). In this analysis, the hepatic blood flow and blood volume were not fixed, but were converged within reasonable ranges. The present analysis suggests that the influx process on the sinusoidal membrane of the liver accounts for the *in vivo* excretion of BQ-123.

Shin *et al.* demonstrated that BQ-123 was transported from the liver to the bile by a primary active system on the canalicular membrane (21). This is an essential step in the excretion of BQ-123, since most of the dose was found to be excreted in the bile in unchanged form. However, it does not seem to be the rate-limiting step *in vivo* in rats, because the sinusoidal

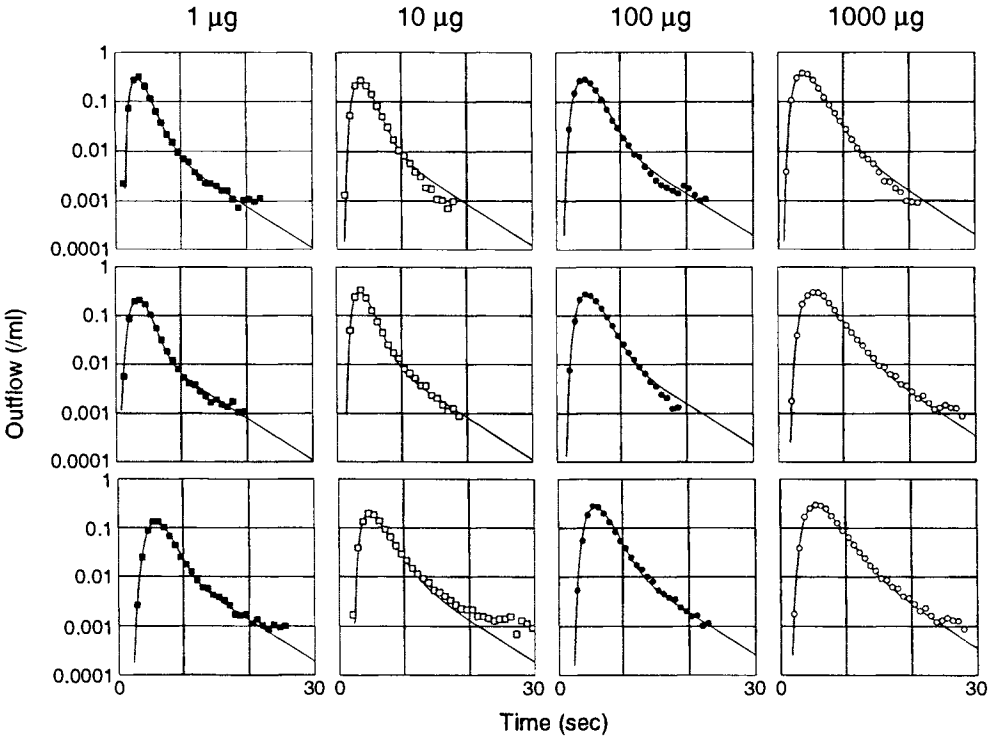

Fig. 2. Schematic representation of least squares fitting analysis of individual dilution curves of BQ-123 to a nonlinear two-compartment dispersion model (Model 4). Calculated parameters are shown in Table 2.

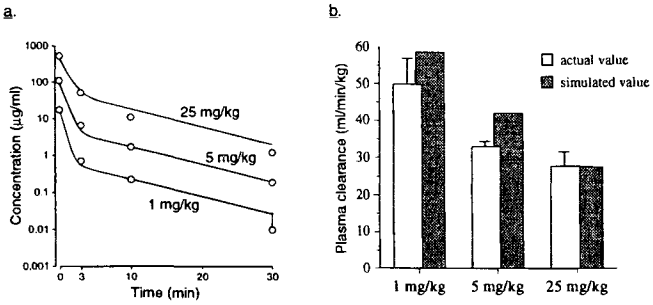

Fig. 3. Least squares fitting analysis of plasma levels of BQ-123 by a hybrid physiological model (a), and actual and simulated plasma clearance of BQ-123 (b), after intravenous injection of the compound in rats. The values of the kinetic parameters obtained from the *in situ* liver perfusion were used for the analysis. See the text for details. Each point represents the mean ± s. d. of three rats. Estimated parameters were Q_H = 58.7 ± 42.6 ml/min/kg, V_B = 82.7 ± 3.9 ml/kg, CL_B = 16.5 ± 5.8 ml/min/kg, and $CL_T V_B/V_T$ = 0.16 ± 0.06 ml/min/kg.

transport explained the *in vivo* hepatic clearance quantitatively as described above. The assumption is supported by the observation that systemic clearance in EHBR rats, whose canalicular transport of BQ-123 is deficient, is almost the same as in normal rats (21).

BQ-123 is monoacidic due to an arginic acid in its structure. There is some evidence that the carrier(s) responsible for the hepatic transport of BQ-123 recognizes the anionic character but not the antagonistic character or the peptidic structure of the compound: the disposition of BQ-123 is influenced by the distribution of endothelin receptors, but only at low concentrations (<10 nM) (27), and the uptake of BQ-123 into isolated hepatocytes is inhibited by the presence of various anions, but is inhibited only weakly by an analogous (but not anionic) peptide (20). It is noteworthy that several studies recently showed that hepatobiliary transport plays a significant role in the pharmacokinetics of various anionic drugs, pravastatin (28), a prostaglandin I_2 agonist (29), and quinolone antibiotics (30).

In the present study, the dispersion model was useful in constructing a systematic view of *in vitro*, *in situ* and *in vivo* events. However, we must caution that the dispersion number calculated by the dispersion model may contain some errors,

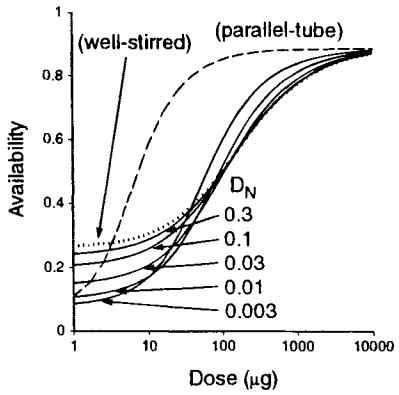

Fig. 4. Effect of the change in normalized dispersion number on the prediction of hepatic availability of BQ-123 after bolus input by the dispersion model. The dotted line and the broken line represent predictions by the well-stirred and parallel tube model, respectively.

because the dispersion assumed in the dispersion model is not physical diffusion but the extent of blood mixing determined primarily by the structure of the micro-capillaries (6,23). The dispersion model hypothesizes that dilution occurs solely by blood mixing; however, in reality dilution is ascribable to both mixing and segregation of the blood flow (20). For this reason, we simulated the effect of change in the dispersion number on the hepatic availability of BQ-123 (Fig. 4). The simulation indicated that several-fold changes in the dispersion number had only a minor influence on the availability, suggesting robustness of the analysis.

In conclusion, we have shown that the extent of saturation of BQ-123 uptake observed *in vitro* (isolated hepatocytes), *in situ* (liver perfusion), and *in vivo* (plasma levels) was in excellent accord. It thus seems reasonable to conclude that carrier-mediated uptake on the sinusoidal membrane of hepatocytes accounts for the *in vivo* excretion of BQ-123 in rats. The nonlinear dispersion model offers reasonable predictions of hepatic availability and *in vivo* plasma disappearance of BQ-123.

REFERENCES

1. C. A. Goresky. Kinetic interpretation of hepatic multiple-indicator dilution studies. *Am. J. Physiol.* **245**:G1–G12 (1983).
2. S. C. Tsao, Y. Sugiyama, Y. Sawada, S. Nagase, T. Iga, and M. Hanano. Effect of albumin on hepatic uptake of warfarin in normal and analbuminemic mutant rats: analysis by multiple indicator dilution method. *J. Pharmacokin. Biopharm.* **14**:51–64 (1986).
3. W. P. Geng, A. J. Schwab, C. A. Goresky, and K. S. Pang. Carrier-mediated uptake and excretion of bromosulfophthalein-glutathione in perfused rat liver: a multiple indicator dilution study. *Hepatology.* **22**:1188–1207 (1995).
4. S. Miyauchi, Y. Sawada, T. Iga, M. Hanano, and Y. Sugiyama. Dose-dependent hepatic handling of l-propranolol determined by multiple indicator dilution method: Influence of tissue binding of l-propranolol on its hepatic elimination. *Biol. Pharm. Bul.* **16**:1019–1024 (1993).
5. C. A. Goresky, G. G. Bach, and C. P. Rose. Effects of saturating metabolic uptake on space profiles and tracer kinetics. *Am. J. Physiol.* **244**:G215–G232 (1983).
6. C. M. Malcorps, C. A. Dawson, J. H. Linehan, T. A. Bronikowski, D. A. Rickaby, A. G. Herman, and J. A. Will. Lung serotonin uptake kinetics from indicator-dilution and constant-infusion methods. *J. Appl. Physiol.* **57**:720–730 (1984).
7. M. S. Roberts, J. D. Donaldson, and M. Rowland. Models of hepatic elimination: comparison of stochastic models to describe residence time distributions and to predict the influence of drug distribution, enzyme heterogeneity, and systemic recycling on hepatic elimination. *J. Pharmacokin. Biopharm.* **16**:41–83 (1988).
8. L. Bass, M. S. Roberts, and P. J. Robinson. On the relation between extended forms of the sinusoidal perfusion and of the convection-dispersion models of hepatic elimination. *J. Theor. Biol.* **126**:457–482 (1987).
9. M. S. Roberts and M. Rowland. Hepatic elimination — dispersion model. *J. Pharm. Sci.* **74**:585–587 (1985).
10. M. S. Roberts and M. Rowland. A dispersion model of hepatic elimination. 1. Formulation of the model and bolus considerations. *J. Pharmacokin. Biopharm.* **14**:227–260 (1986).
11. Y. Yano, K. Yamaoka, Y. Aoyama, and H. Tanaka. Two-compartment dispersion model for analysis of organ perfusion system of drugs by fast inverse Laplace transform (FILT). *J. Pharmacokin. Biopharm.* **17**:179–202 (1989).
12. Z. A. Hussein, J. McLachlan, and M. Rowland. Distribution kinetics of salicylic acid in the isolated perfused rat liver assessed using moment analysis and the two-compartment axial dispersion model. *Pharm. Res.* **11**:1337–1345 (1994).
13. B. A. Saville, M. R. Gray, and Y. K. Tam. Models of hepatic drug elimination. *Drug Metab. Rev.* **24**:49–88 (1992).

14. A. Hisaka and Y. Sugiyama. Analysis of nonlinear and non-steady state hepatic extraction with the dispersion model using the finite difference method. *J. Pharmacokin. Biopharm.* 26: in press.
15. C. A. Poulain, B. A. Finlayson, and J. B. Bassingthwaighte. Efficient numerical methods for nonlinear-facilitated transport and exchange in a blood-tissue exchange unit. *Ann. Biomed. Eng.* **25**:547–564 (1997).
16. M. Ihara, K. Noguchi, T. Saeki, T. Fukuroda, S. Tsuchiya, S. Kimura, T. Fukami, K. Ishikawa, M. Nishikibe, and M. Yano. Biological profiles of highly potent novel endothelin antagonists selective for the ETA receptor. *Life Sci.* **50**:247–255 (1992).
17. E. H. Ohlstein, A. Arleth, H. Bryan, J. D. Elliott, and C. P. Sung. The selective endothelin ETA receptor antagonist BQ123 antagonizes endothelin-1-mediated mitogenesis. *Eur. J. Pharmacol.* **259**:339–342 (1994).
18. S. Ito, K. Ide, and T. Sasaki. Role of endothelin-1 and ETA receptor in delayed cerebral vasospasm following subarachnoid hemorrhage. *Can. J. Neurol. Sci.* **20**:S14 (1993).
19. M. Okada, T. Fukuroda, K. Shimamoto, R. Takahashi, F. Ikemoto, M. Yano, and M. Nishikibe. Antihypertensive effects of BQ-123, a selective endothelin ETA receptor antagonist, in spontaneously hypertensive rats treated with Doca-salt. *Eur. J. Pharmacol.* **259**: 339–342 (1994).
20 T. Nakamura, A. Hisaka, Y. Sawasaki, Y. Suzuki, T. Fukami, K. Ishikawa, M. Yano, and Y. Sugiyama. Carrier-mediated active transport of peptidic endothelin antagonist BQ-123 into rat hepatocytes. *J. Pharmacol. Exp. Ther.* **278**:564–572 (1996).
21. H. Shin, Y. Kato, T. Yamada, A. Hisaka, and Y. Sugiyama. Hepatobiliary transport mechanism for the cyclopentapeptide endothelin antagonist BQ-123. *Am. J. Physiol.* **278**:607–613 (1996).
22. C. C. Paulusma, P. J. Bosma, G. J. R. Zaman, C. T. M. Bakker, G. L. Sceffer, R. J. Scheper, P. Borst, and R. P. J. Oude Elferink. Congenital jaundice in rats with a mutation in a multidrug resistance-associated protein gene. *Science* **271**:1126–1128 (1996).
23. K. Ito, H. Suzuki, T. Hirohashi, K. Kume, T. Shimizu, and Y. Sugiyama. Molecular cloning of canalicular multispecific organic anion transporter defective in EHBR. *Am. J. Physiol.* **262**:G16–G22 (1997).
24. M. Buchler, J. Konig, M. Brom, J. Kartenbeck, H. Spring, T. Horie, and D. Keppler. cDNA cloning of the hepatocyte canalicular isoform of the multidrug resistance protein, cMrp, reveals a novel conjugate export pump deficient in hyperbilirubinemic mutant rats. *J. Biol. Chem.* **271**:15091–15098 (1996).
25. H. Akaike. A new look at the statistical model identification. *IEEE Trans. Automat. Control* **19**:716–723 (1974).
26. M. Nishimura, K. Yamaoka, S. Naito, and T. Nakagawa. Hepatic local disposition of a drug with high protein binding and high hepatic clearance using BOF-4272 as a model drug. *Biol. Pharm. Bull.* **19**:1197–1202 (1996).
27. H. Shin, Y. Kato, Y. Shitara, T. Yamada, T. Nakamura, A. Hisaka, and Y. Sugiyama. The endothelin receptor is a major determinant for the nonlinear tissue distribution of the endothelin antagonist BQ-123, *J. Pharmacol Exp. Ther.* **278**:607–613 (1996).
28. M. Yamazaki, S. Akiyama, R. Nishigaki, and Y. Sugiyama. Uptake is the rate-limiting step in the overall hepatic elimination of pravastatin at steady-state in rats. *Pharm. Res.* **13**:1559–1564 (1996).
29. H. Imawaka and Y. Sugiyama. Kinetic study of the hepatobiliary transport of a new prostaglandin receptor agonist. *J. Pharmacol. Exp. Ther.* **284**:949–957 (1998).
30. H. Sasabe, T. Terasaki, A. Tsuji, and Y. Sugiyama. Carrier-mediated hepatic uptake of quinolone antibiotics in the rat. *J. Pharmacol. Exp. Ther.* **282**:162–171 (1997).